

Supporting Information

An Activator-Blocker Pair Provides a Controllable On-Off Switch for a Ketosteroid Isomerase Active Site Mutant

Vandana Lamba[†], Filip Yabukarski[†] and Daniel Herschlag^{*,†,‡,§}

[†]Department of Biochemistry, Stanford University, Stanford, California 94305, United States

[‡]Department of Chemistry, Stanford University, Stanford, California 94305, United States

[#]Department of Chemical Engineering, Stanford University, Stanford, California 94305, United States

[§]Stanford ChEM-H, Stanford University, Stanford, California 94305, United States

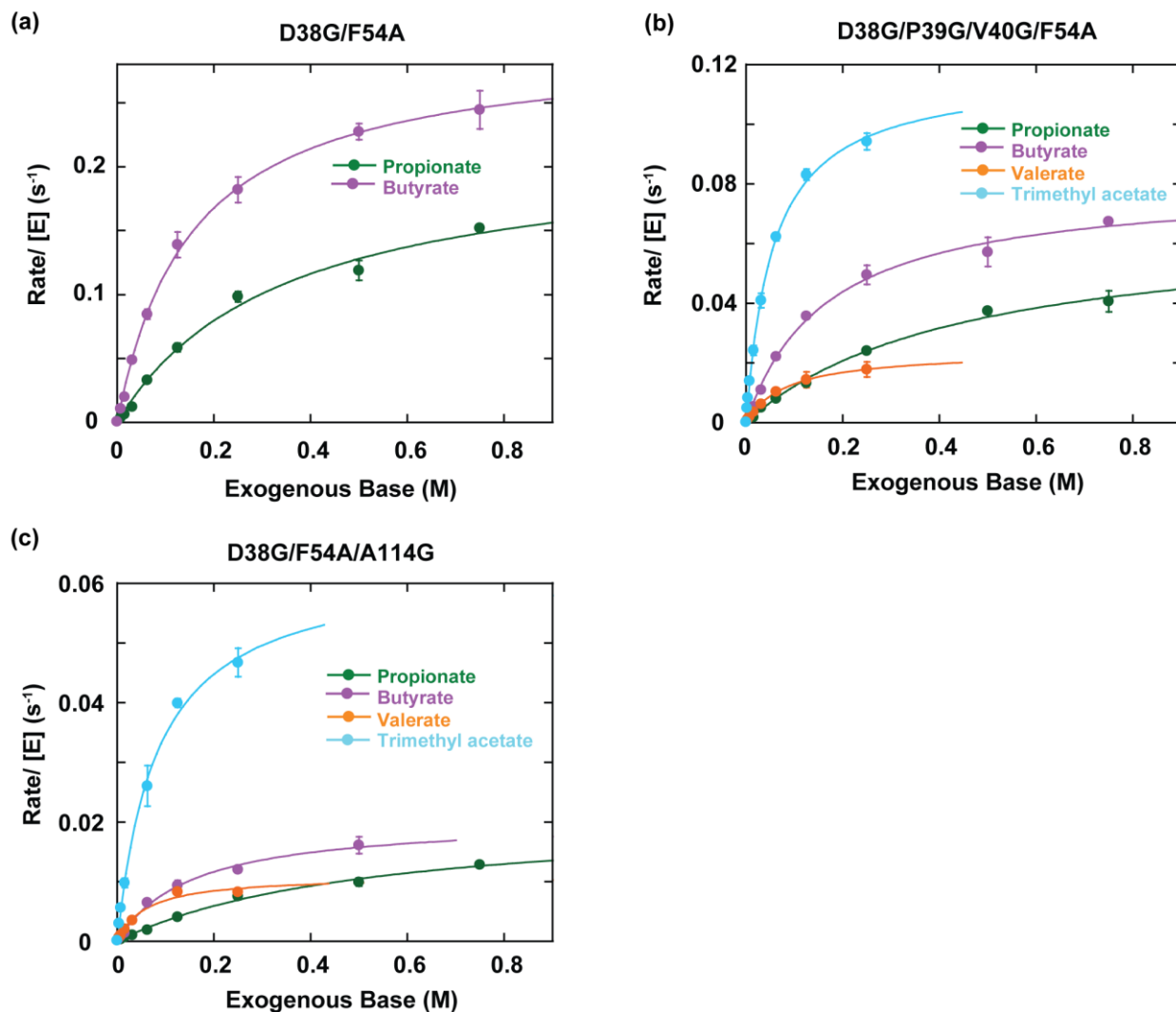


Figure S1. Rescue reactions for exogenous bases in tKSI mutants with the F54A mutation. Data were obtained as described in Experimental Section (“KSI Mutants Base Rescued Reactions”) and fit to the Michaelis-Menten equation. Error bars show standard deviations from 2-3 independent experiments using different enzyme concentrations varied from 0.25 to 1.5 μM . The first-order rate constants $k_{\text{cat,EB}}$ and $K_{\text{M,base}}$ (defined in Scheme S2) of the exogenous bases are given in Table S1 along with the associated errors.

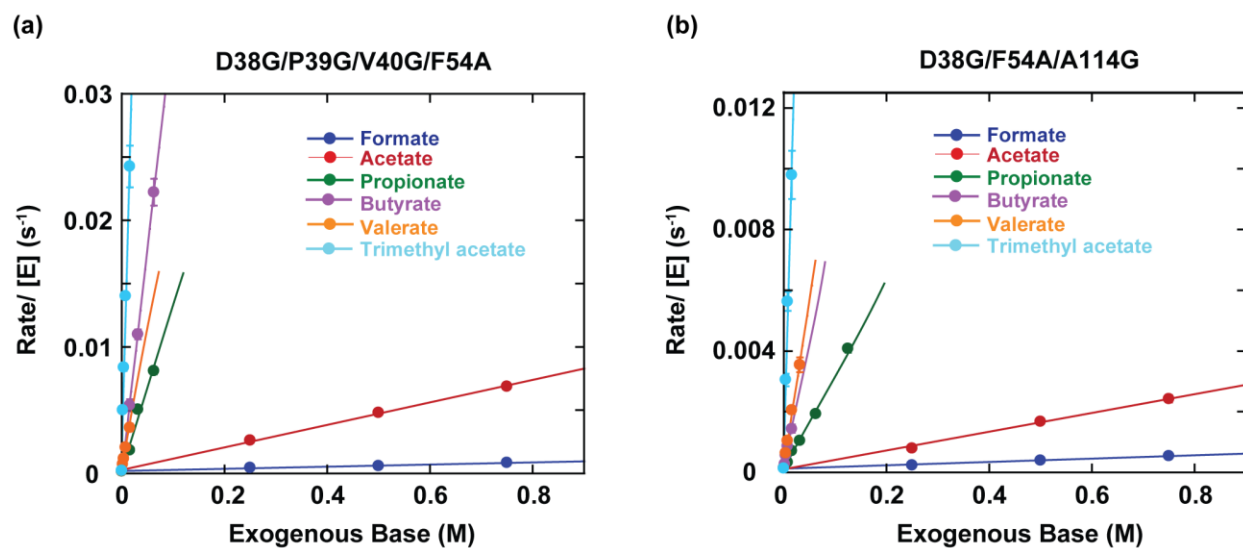


Figure S2. Rescue reactions for exogenous bases in tKSI mutants with the F54A mutation. Data were obtained as described in Experimental Section (“KSI Mutants Base Rescued Reactions”) and fit to a linear equation. Error bars show standard deviations from 2-3 independent experiments using different enzyme concentrations varied from 0.25 to 1.5 μ M. The values for second-order rate constants and associated errors are given in Table S1.

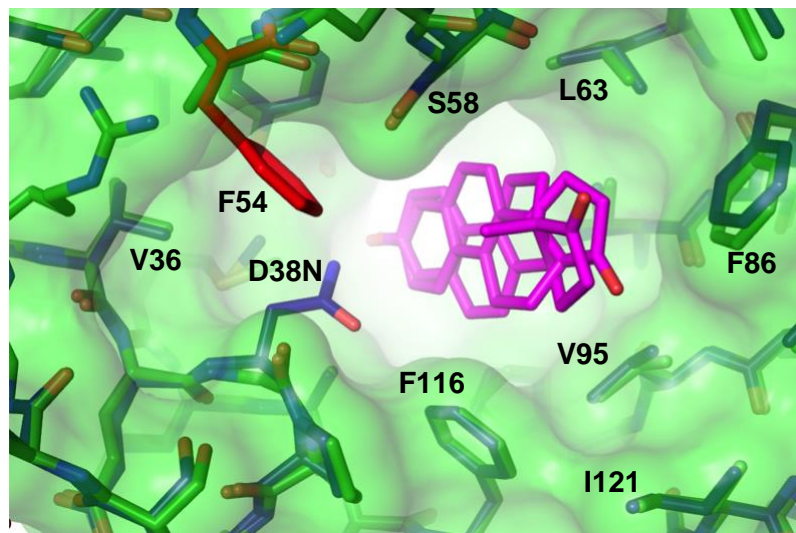


Figure S3. The D38G/F54A cavity shown with residues lining the cavity. D38G/F54A shown in green (surface and stick representation of residues; PDB: 5UGI) with bound equilenin (purple) and is aligned with D38N structure (stick representation of residues in blue; PDB:1QJG). F54 (red) and D38N (blue) from the D38N structure are shown to illustrate the position they occupy when present and the space opened upon introducing these mutations in D38G/F54A. Representative surrounding residues to the cavity are shown to illustrate the conservation of the overall structure in D38G/F54A.

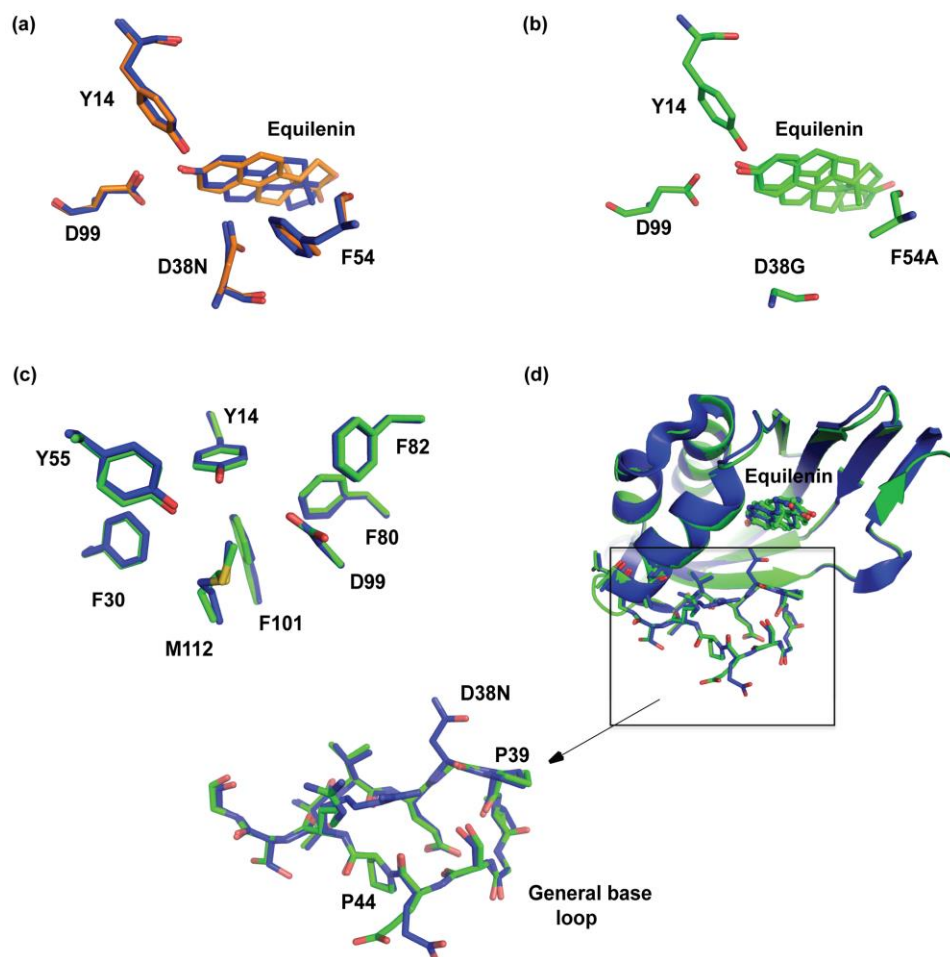


Figure S4. Structural comparison of D38G/F54A tKSI (green; PDB: 5UGI; this work) with D38N tKSI (blue; PDB: 1QJG) with bound equilenin, a transition state analog. (a, b) Active site residues and bound equilenin in D38N (a: sticks shown in blue and orange represent two orientations of equilenin as observed in two crystallographically independent protein chains (blue and orange) in the asymmetric unit of the D38N crystal) and D38G/F54A (b: sticks in green show the two alternative orientations of equilenin modeled). (c) Overlay of the oxyanion hole of D38G/F54A (green) and D38N (blue). (d) Overlay of the overall structures of D38G/F54A (green) and D38N tKSI (blue), with an RMSD of 0.35 Å for the backbone atoms. The inset shows local structure around the sites of mutation in the general base loop region.

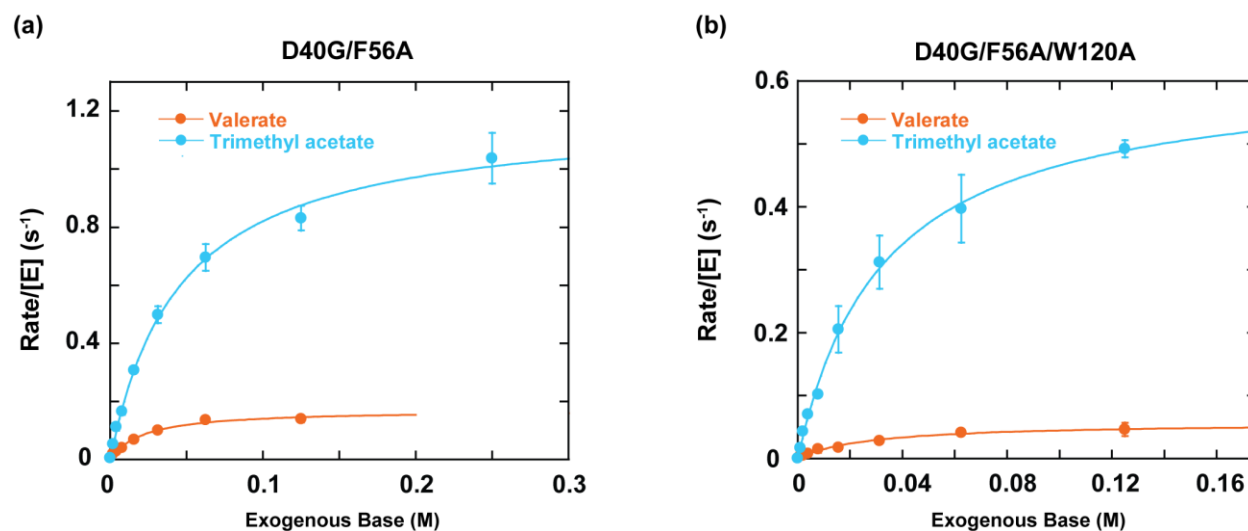


Figure S5. Rescue reactions for exogenous bases in pKSI mutants with the F56A mutation. Data were obtained as described in Experimental Section (“KSI Mutants Base Rescued Reactions”) and fit to the Michaelis-Menten equation. Error bars show standard deviations from 2-3 independent experiments using different enzyme concentrations varied from 0.25 μ M to 1.5 μ M. The first-order rate constants $k_{\text{cat,EB}}$ and $K_{\text{M,base}}$ (defined in Scheme S2) of the exogenous bases are given in Table S3 along with the associated errors.

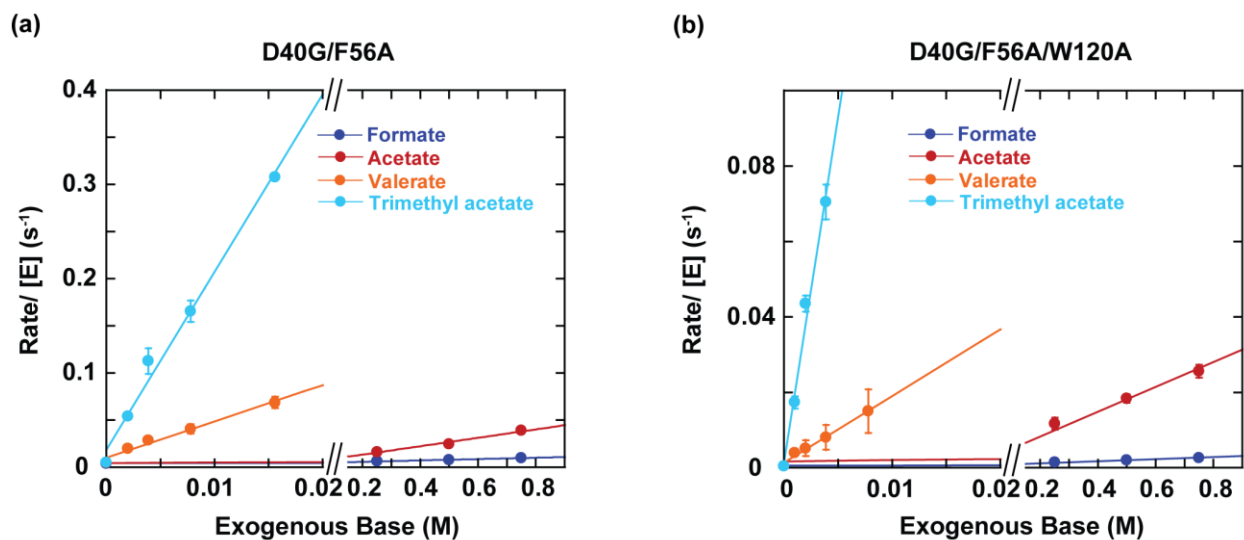


Figure S6. Rescue reactions for exogenous bases in pKSI mutants with the F56A mutation. Data were obtained as described in Experimental Section (“KSI Mutants Base Rescued Reactions”) and fit to a linear equation. Error bars show standard deviations from 2-3 independent experiments using different enzyme concentrations varied from 0.25 to 1.5 μ M. The values for second-order rate constants and associated errors are given in Table S3.

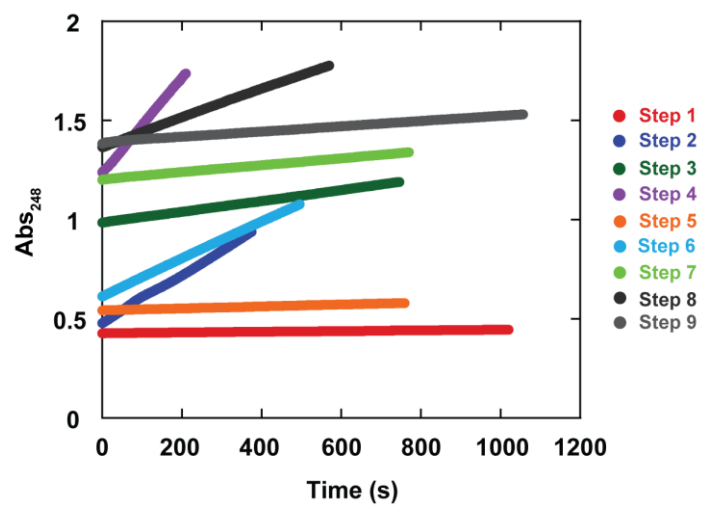


Figure S7. Measured absorbance traces for “Turning KSI On and Off” (see Experimental Section in main text).

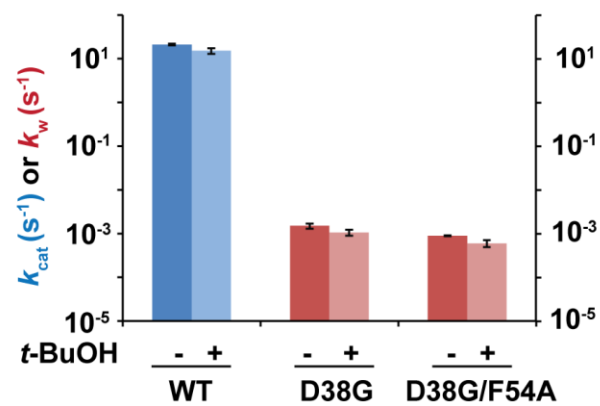


Figure S8. Activity effects of *t*-BuOH (250 mM) on WT and mutant tKSI enzymes in the absence of a rescuing base.

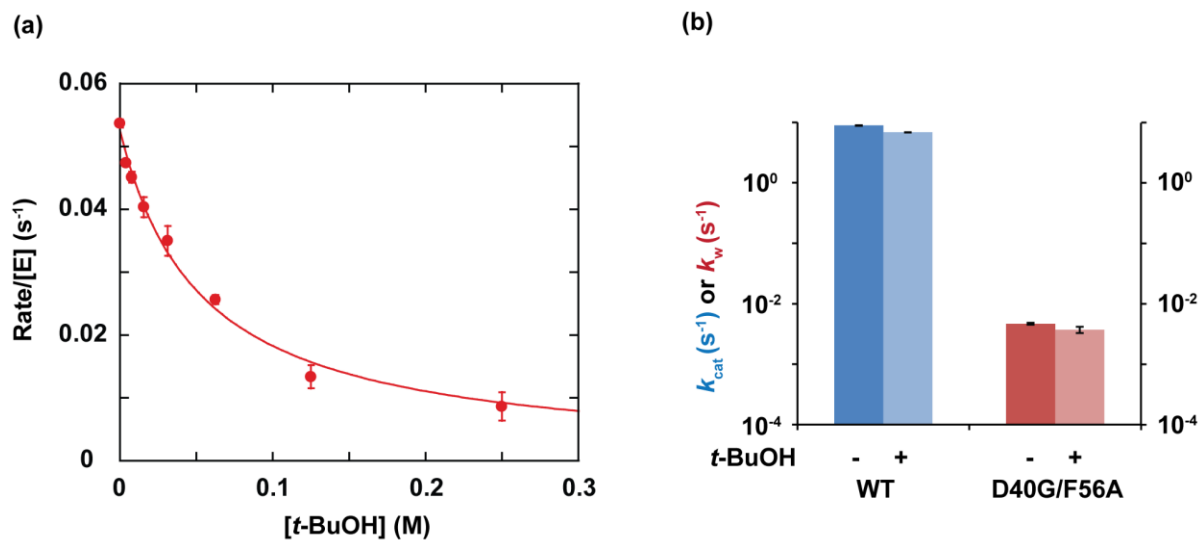


Figure S9. Inhibition of base rescue in pKSI by *t*-BuOH. (a) As for tKSI mutant, *t*-BuOH inhibited the TMA (2 mM) rescued reaction in D40G/F56A pKSI, and gives $K_i = 53 \pm 5$ mM, similar to the $K_{\text{M,base}}$ of 45 ± 4 mM for TMA rescue (Table S3). (b) *t*-BuOH (250 mM) had no significant effects on the activity of WT pKSI or the water reaction (i.e., non-base rescued) of D40G/F56A.

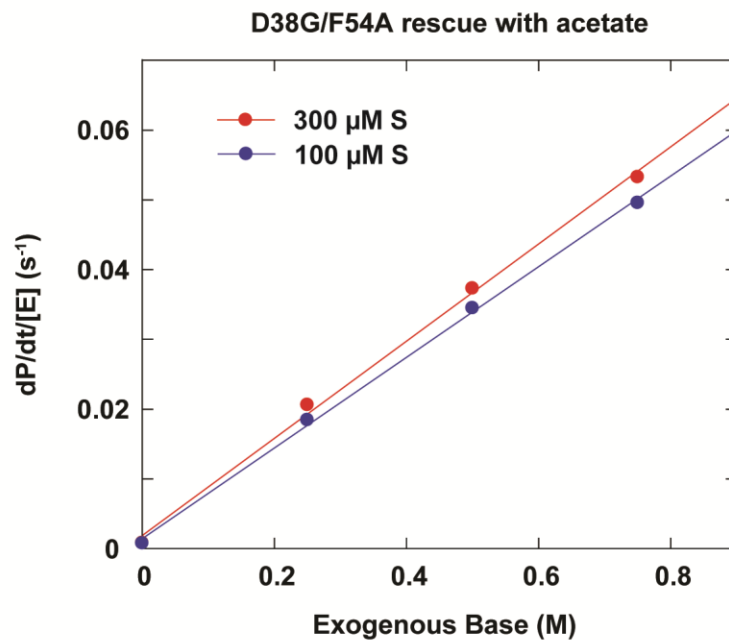
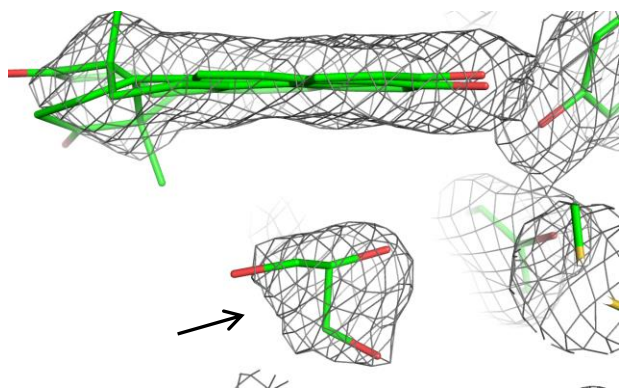


Figure S10. Rescue of D38G/F54A tKSI with acetate at two different substrate concentrations of 5(10)-EST. The second-order rate constants at near-saturating substrate concentrations of 300 μM (●) and 100 μM (●) (both above the $K_{M,S}$ of 19 μM ; Ref. 33) give $k_{\text{base}} = 7.0 \times 10^{-2}$ and $6.5 \times 10^{-2} \text{ M}^{-1} \text{ s}^{-1}$, respectively.

(a)



(b)

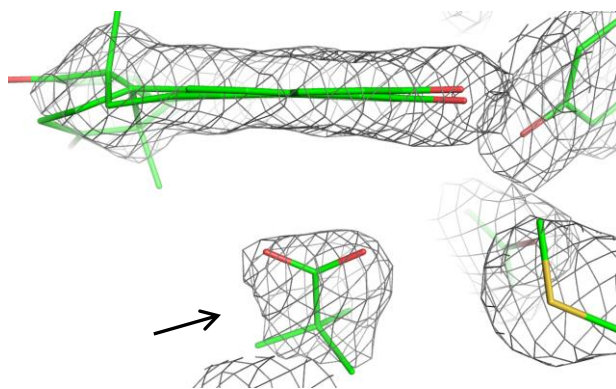


Figure S11. Modeling of additional electron density (arrow) in D38G/F54A structure for a glycerol (a) or TMA molecule (b).

Table S1. Rate Constants for tKSI General Base Mutants with Exogenous Bases

Mutant	Exogenous Base	$k_{cat,EB}$ (10^{-2} s^{-1})	$K_{M,base}$ (mM)	k_{base} ($10^{-2} \text{ M}^{-1} \text{ s}^{-1}$)
D38G	Formate		>750	1.2 ± 0.3^a
	Acetate		>750	0.6 ± 0.1^a
	Propionate		>750	0.3 ± 0.1^a
	Butyrate		>750	$<0.1^a$
	Valerate		>250	$<0.3^a$
	TMA		>250	$<0.3^a$
D38G/F54A	Formate		>750	
	Acetate		>750	7.0 ± 0.6^a
	Propionate	22 ± 2	340 ± 60	36 ± 1^a
	Butyrate	30 ± 1	150 ± 9	140 ± 7^a
	Valerate	15 ± 1	60 ± 7	180 ± 20^a
	TMA	110 ± 7	68 ± 10	1100 ± 90^a
D38G/P39G/V40G/F54A	Formate		>750	0.08 ± 0.01
	Acetate		>750	0.9 ± 0.02
	Propionate	6.7 ± 0.5	450 ± 60	13 ± 1
	Butyrate	8.1 ± 0.3	170 ± 20	35 ± 0.4
	Valerate	2.4 ± 0.04	84 ± 3	22 ± 1
	TMA	12 ± 0.2	56 ± 3	150 ± 10
D38G/F54A/A114G	Formate		>750	0.06 ± 0.004
	Acetate		>750	0.3 ± 0.01
	Propionate	2.1 ± 0.2	520 ± 80	3.1 ± 0.1
	Butyrate	2.1 ± 0.1	150 ± 20	8.4 ± 0.5
	Valerate	1.1 ± 0.1	60 ± 14	11 ± 0.4
	TMA	6.3 ± 0.3	83 ± 9	61 ± 4

Conditions: 20 mM sodium MOPS, pH 7.2, 2% DMSO, ionic strength 1 M (NaCl). Data were collected as described in Experimental Section (“KSI Mutants Base Rescued Reactions”). The first-order rate constants $k_{cat,EB}$ and $K_{M,base}$ (defined in Scheme S2) values for exogenous bases and errors associated with them were obtained from nonlinear least squares fits to data shown in Figure S1. Using only low base concentration points devoid of any significant saturation behavior, values of second-order rate constants, k_{base} , were obtained by linear least squares fits of the data shown in Figure S2. The second-order rate constants k_{base} can also be obtained by dividing $k_{cat,EB}$ and $K_{M,base}$. These k_{base} values (not shown) are within two fold of the values reported here by linear fits. The lower limit of $K_{M,base}$ value is given as the highest concentration of the base used in the study where no significant deviation from linearity was observed.

^a Values from Ref. 33.

Table S2. Crystallographic Data Collection and Refinement Statistics

	D38G/F54A + Equilenin
Data collection	
Space group	P6 ₅ 22
Cell dimensions	
<i>a</i> , <i>b</i> , <i>c</i> (Å)	60.78 60.78 143.09
α , β , γ (°)	90.00 90.00 120.00
Resolution (Å)	35.34 – 1.80 (1.84 – 1.80) *
<i>R</i> _{sym} or <i>R</i> _{merge}	0.072 (2.688)**
<i>I</i> / σI	18.4 (1.0)
Completeness (%)	100 (99.5)
Redundancy	12.1 (12.3)
Refinement	
Resolution (Å)	35.34 – 1.80
No. reflections	15307
<i>R</i> _{work} / <i>R</i> _{free}	0.179 / 0.227
No. atoms	
Protein	1098
Ligand/ion	40
Water	86
<i>B</i> -factors	
Protein	42.38
Ligand/ion	41.04
Water	45.80
R.m.s. deviations	
Bond lengths (Å)	0.005
Bond angles (°)	0.72

* Values in parentheses are for highest-resolution shell.

** Higher multiplicity contributes to higher *R*_{merge} values.

Table S3. Rate Constants for pKSI General Base Mutants with Exogenous Bases

Mutant	Exogenous Base	$k_{cat,EB}$ (10^{-2} s^{-1})	$K_{M,base}$ (mM)	k_{base} ($10^{-2} \text{ M}^{-1} \text{ s}^{-1}$)
D40G/F56A	Formate		>750	0.73 ± 0.04
	Acetate		>750	4.5 ± 0.3
	Valerate	17 ± 1	22 ± 3	390 ± 30
	TMA	120 ± 3	45 ± 4	1900 ± 120
D40G/F56A/W120A	Formate		>750	0.28 ± 0.03
	Acetate		>750	3.3 ± 0.3
	Valerate	5.7 ± 0.4	28 ± 5	180 ± 10
	TMA	62 ± 2	33 ± 2	1800 ± 160

Conditions: 20 mM sodium MOPS, pH 7.2, 2% DMSO, ionic strength 1 M (NaCl). Data were collected as described in Experimental Section (“KSI Mutants Base Rescued Reactions”). The first-order rate constants $k_{cat,EB}$ and $K_{M,base}$ (defined in Scheme S2) values for exogenous bases and errors associated with them were obtained from nonlinear least squares fits to data shown in Figure S5. Using only low base concentration points devoid of any significant saturation behavior, values of second-order rate constants, k_{base} , were obtained by linear least squares fits of the data shown in Figure S6. The second-order rate constants k_{base} can also be obtained by dividing $k_{cat,EB}$ and $K_{M,base}$. These k_{base} values (not shown) are within two fold of the values reported here by linear fits. For formate and acetate, the lower limit of $K_{M,base}$ value is given as the highest concentration of the base used in the study where no significant deviation from linearity was observed.

Table S4. Effective Molarity of General Base in tKSI and pKSI for TMA Rescue of General Base Binding Pocket Mutants

(A)

Mutant Enzyme	Exogenous Base	WT k_{cat} (s^{-1})	k_{base} ($10^{-2} \text{ M}^{-1} \text{ s}^{-1}$)	Effective Molarity (M)
tKSI D38G/F54A	TMA	36 ^a	1100	3
pKSI D40G/F56A	TMA	9.9 ^b	1900	0.5

(B)

Mutant Enzyme	Exogenous Base	WT $k_{\text{cat}}/K_{\text{M}}$ ($10^5 \text{ M}^{-1} \text{ s}^{-1}$)	$k_{\text{base}}/K_{\text{M,S}}$ ($10^5 \text{ M}^{-2} \text{ s}^{-1}$)	Effective Molarity (M)
tKSI D38G/F54A	TMA	7.2 ^a	5.7	1.3
pKSI D40G/F56A	TMA	5.4 ^b	9.5	0.6

k_{base} values for tKSI and pKSI mutants are from Tables S1 and S3 respectively. $K_{\text{M,S}}$ values obtained from water rescued reactions for tKSI and pKSI mutants were used and are from Ref. 33 and Table S8, respectively.

^a Values from Ref. 37.

^b Values from Ref. 36.

Table S5. Observed and Predicted Rates for Successively Turning KSI On and Off

Step	Observed Rate/[E] (s ⁻¹)	Predicted Rate/[E] (s ⁻¹)	Observed/Predicted Rate
1	5.9 X 10 ⁻⁴	8.9 X 10 ⁻⁴	0.7
2	4.1 X 10 ⁻²	2.8 X 10 ⁻²	1.5
3	9.2 X 10 ⁻³	5.6 X 10 ⁻³	1.6
4	8.2 X 10 ⁻²	6.2 X 10 ⁻²	1.3
5	1.7 X 10 ⁻²	2.2 X 10 ⁻²	0.8
6	3.2 X 10 ⁻¹	2.2 X 10 ⁻¹	1.5
7	5.9 X 10 ⁻²	4.4 X 10 ⁻²	1.3
8	2.4 X 10 ⁻¹	4.4 X 10 ⁻¹	0.6
9	6.7 X 10 ⁻²	1.7 X 10 ⁻¹	0.4

Observed rates obtained as described in Experimental Section (“Turning KSI On and Off”). See below for predicted rates.

The predicted rate for step 1 is obtained from first-order rate constant k_w of non-base rescued reaction of D38G/F54A (Ref. 33). For step 2, the rate was predicted from second-order rate constant of TMA rescued reaction and using equation 1.

$$\text{Rate} = k_{\text{TMA}} [\text{TMA}] [\text{E}\cdot\text{S}]. \quad (1)$$

As 300 μM substrate was used, a value well above the $K_{\text{M,S}}$ of 19 μM , $[\text{E}\cdot\text{S}]$ is nearly equal to $[\text{E}]_{\text{total}}$ and replaced with it for the predicted calculation. For the next two steps, the rates were predicted using the equation 2.

$$\text{Rate}/[\text{E}] = (\text{Rate}_{\text{max}}/[\text{E}]) / (1 + [\text{I}]/K_i^{\text{obsd}}). \quad (2)$$

For step 3, $\text{Rate}_{\text{max}}/[\text{E}]$ is the predicted $\text{Rate}/[\text{E}]$ from step 2, as we are inhibiting the step 2 reaction from 2.5 mM TMA with 250 mM *t*-BuOH in this step. As this TMA concentration is not saturating, $K_i^{\text{obsd}} = 63$ mM was used to obtain the predicted rate. Step 4 involved reaction of 28 mM TMA (2.5 mM TMA (step 1) + additional 25 mM (step 4)) in the presence of 250 mM *t*-BuOH, with the predicted rate calculated as follows. As 28 mM, TMA is subsaturating ($K_{\text{M,base}} = 68$ mM in D38G/F54A tKSI; Supporting Information, Table S1), we used equation (1) to obtain Rate_{max} and the K_i^{obsd} of 63 mM for *t*-BuOH inhibition to predict the observed rate. In step 5,

which involves 0.2 μ M enzyme and 2.8 mM TMA in presence of 25 mM *t*-BuOH (from the 10 fold dilution in step 5 from the step 4 conditions), Rate_{max} was calculated using equation (1) and $K_i^{\text{obsd}} = 63$ mM for inhibition with *t*-BuOH was used. The predicted rate was calculated using equation (2). Step 6 involved reaction of 28 mM TMA (2.8 mM TMA (step 5) + additional 25 mM (step 6)) in the presence of 25 mM *t*-BuOH (step 5), Rate_{max} was calculated using equation (1) and predicted rate was obtained using equation (2) with a K_i^{obsd} of 63 mM for *t*-BuOH inhibition. In step 7, we inhibited the reaction of step 6 by adding 250 mM *t*-BuOH. Therefore, the rate of step 6 was used as Rate_{max} and with a K_i^{obsd} of 63 mM for *t*-BuOH inhibition; we obtained the predicted rate using equation (2). For step 8, Rate_{max} was approximated as k_{cat} of saturated base reaction, as 128 mM TMA (28 mM (step 6) + 100 mM (step 8)) is nearly two fold more than the $K_{\text{M,base}}$ of 68 mM for TMA. At this TMA concentration, K_i^{obsd} for *t*-BuOH was estimated using equation (3), and equation (2) was used to obtain the predicted value.

$$K_i = K_i^{\text{obsd}} / (1 + [\text{TMA}] / K_{\text{M}}^{\text{TMA}}). \quad (3)$$

Step 9 involves reaction of 125 mM TMA in presence of 1 M *t*-BuOH. As TMA concentration is higher than its $K_{\text{M,base}}$ of 68 mM, Rate_{max} was approximated as k_{cat} of saturated base reaction. K_i^{obsd} for *t*-BuOH at 125 mM TMA was estimated using equation (3), and predicted rate was obtained using equation (2).

Table S6. Observed and Calculated Inhibition Constants for *t*-BuOH

TMA (mM)	$K_i^{\text{obsd, } t\text{-BuOH}}$ (mM)	$K_i^{t\text{-BuOH}}$ (mM)
2	63 ± 4	63
75	140 ± 20	67
250	270 ± 30	58

Conditions: 20 mM sodium MOPS, 2% DMSO, pH 7.2, *t*-BuOH (0-250 mM), 1 M ionic strength (NaCl). The values for K_i^{obsd} are from Figure 4. Competitive inhibition of TMA rescued reaction with *t*-BuOH is defined in Scheme S2 and K_i of *t*-BuOH was obtained from observed K_i values using the equation: $K_i = K_i^{\text{obsd}} / (1 + [\text{TMA}] / K_M^{\text{TMA}})$.

Table S7. Fold Rate Enhancement in D38G/F54A tKSI Activity with Saturating Exogenous Base

Exogenous Base	k_w (s^{-1})	$k_{cat,EB}$ (s^{-1})	$k_w / k_{cat,EB}$
Valerate	8.9×10^{-4}	0.15	170
TMA	8.9×10^{-4}	1.13	1300

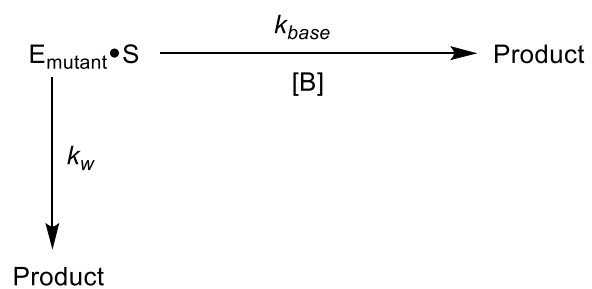
The rate constants k_w and $k_{cat,EB}$ are defined in Schemes S1 and S2. Value of k_w and $k_{cat,EB}$ are from Ref. 33 and Table S1 respectively.

Table S8. Michaelis-Menten Parameters of tKSI and pKSI General Base Mutants with 5(10)-EST Substrate for Reactions in the Absence of a Rescuing Base

Mutant	k_w (10^{-4} s^{-1})	$K_{M,S}$ (μM)	$k_w/K_{M,S}$ ($\text{M}^{-1} \text{ s}^{-1}$)
D38G/P39G/V40G/F54A	2.1 ± 0.1	52 ± 7	3.0 ± 0.2
D38G/F54A/A114G	1.7 ± 0.2	73 ± 17	1.6 ± 0.2
D40G/F56A	52 ± 3	20 ± 4	247 ± 30
D40G/F56A/W120A	4.0 ± 0.8	77 ± 6	5.8 ± 0.4

Conditions: 4 mM sodium phosphate, 2% DMSO, pH 7.2. Data were obtained as described in Experimental Section (“KSI Mutants Non-Base Rescued Reactions”). The rate constant k_w is defined in Scheme S1. The values of k_w and $K_{M,S}$ and errors associated with them were obtained from non-linear least squares fit of the data. Using only low substrate concentration points devoid of any saturation behavior, values of second-order rate constants $k_w/K_{M,S}$ were obtained by linear least squares fit of the data. The $k_w/K_{M,S}$ values obtained by dividing k_w and $K_{M,S}$ (not shown here) are within two fold of values reported from linear fits.

Scheme S1: KSI General Base Mutant Reactions



Scheme S2: Inhibition of Base-Rescued Reaction in KSI General Base Mutant

